

Fig. 1: (left) Typical kinematical range of data used in nPDF global analysis with addition of W/Z pPb LHC data. (right) Example kinematical range of data used in free-proton PDF global analysis [1].

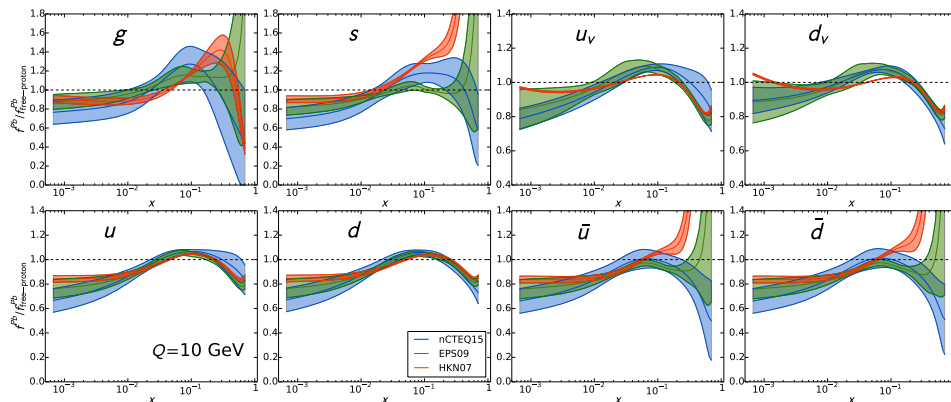


Fig. 2: Comparison of lead nuclear modifications,  $R_i^{Pb} = \frac{f_i^{Pb}}{f_i^{\text{free-proton}}}$ , obtained by nCTEQ15 [2], EPS09 [3] and HKN07 [4] nPDF global analyses. Figure from [2].

main practical differences between the proton and nuclear PDF fits. This is illustrated in Fig. 1 where we compare the kinematical range of data in both cases. The lack of data is also the reason why in many cases additional assumptions need to be introduced in the nPDF analyses in order to obtain stable fits. This necessity, however, can lead to sizable differences (much bigger than for proton PDFs) between different nPDFs, see Fig. 2.

Vector boson production in hadron collisions is a very well understood process and serves as one of the “standard candle” measurements at the LHC.  $W^\pm$  and  $Z$  bosons are numerous produced in heavy ion proton-lead (pPb) and lead-lead (PbPb) collisions at the LHC and can be used to gain

insight into the structure of nPDFs. As the  $W$  and  $Z$  bosons couple weakly, their interaction with the nuclear medium is negligible which makes these processes one of the cleanest probes of the nuclear structure available at the LHC. The possibility of using vector boson production data to constrain nPDFs was considered before the LHC data were available [5], and this demonstrated a strong potential for the proton-lead data to constrain nPDFs. The current LHC measurements for  $W^\pm$  and  $Z$  production include mostly rapidity distributions for both pPb and PbPb collisions [6–15]. Some of these data were already used in a reweighting analyses [16] and more recently [17] to estimate the impact of these data on EPS09 [3], DSSZ [18] and nCTEQ15 [2] nPDFs. Analysis of these data was also performed within the framework of KP model [19]. Lately, a first global analysis of nPDFs with LHC data, EPPS16 [20], have been published.<sup>1</sup>

In this work we present predictions for vector boson production in pPb and PbPb collisions at the LHC obtained using nCTEQ15 nuclear parton distributions, and perform a comprehensive comparison to the available LHC data. We also identify the measurements which have the biggest potential to constrain the nPDFs with special attention to the strange distribution. Finally, we perform a reweighting study which gives indications on the effects of including these data in the nCTEQ global fit. This proceedings is based on the recent study [17] with additional material on the nuclear strange distribution.

## 2. Comparison to the LHC vector boson data

We start by comparing predictions for vector boson production at the LHC calculated using nCTEQ15 nPDFs [2] to the available experimental data (for the proton beam we use CT10 proton PDFs [22]). In this note we concentrate only on the most relevant data sets, namely  $W^\pm$  production in pPb collisions ( $\sqrt{s} = 5.02$  TeV) from CMS [9] and ATLAS [10]. A more comprehensive comparison with all the currently available vector boson data can be found in ref. [17]. Our calculations are done using next-to-leading order (NLO) with help of FEWZ [23] program.

In Fig. 3 we present results for CMS [9] and ATLAS [10] data. In the plots we show data overlaid with predictions using nCTEQ15 nPDFs (blue band) and additionally we show results obtained with free proton PDFs (yellow band) for which we choose CT10 distributions [22].<sup>2</sup>

In both  $W^+$  and  $W^-$  cases we see a common pattern. The low rapidity ( $y_{l^\pm} < 0$ ) data are well described by the nPDFs, whereas when we go

<sup>1</sup> Interesting scaling properties of the LHC  $W$  production data from pp, pPb and PbPb collisions have been observed in [21].

<sup>2</sup> We include here the isospin effects.

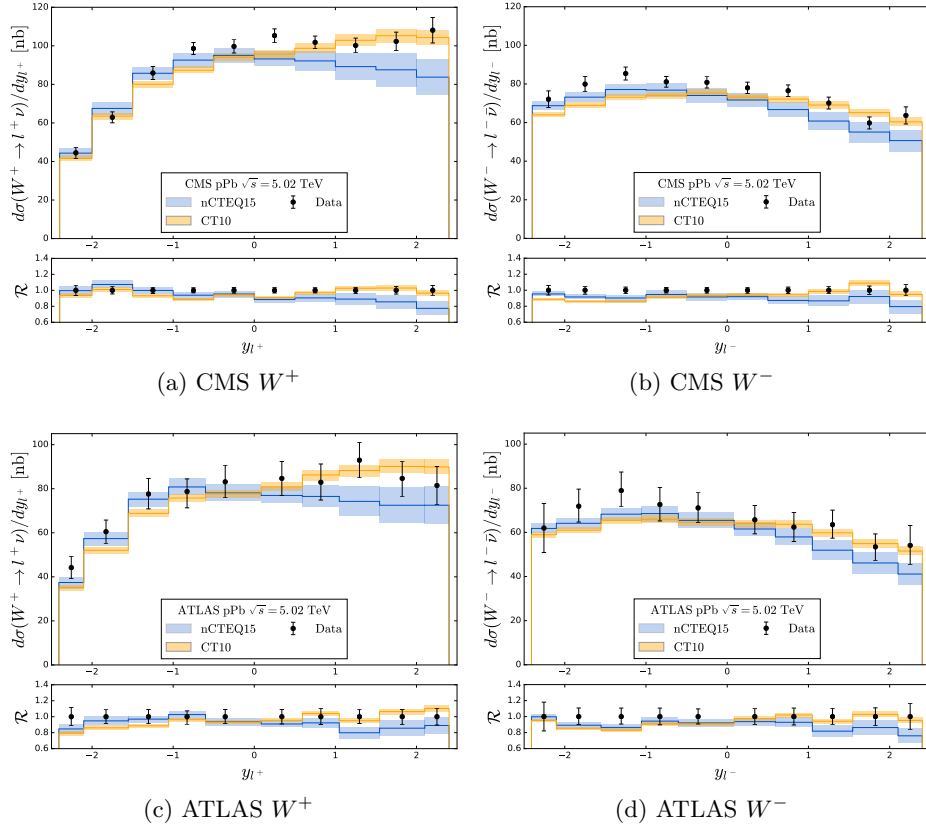


Fig. 3:  $W^\pm$  production in pPb collisions at the LHC from CMS (upper plots) and ATLAS (lower plots) compared with predictions from nCTEQ15 nPDFs and CT10 proton PDFs.

towards larger rapidities ( $y_{l^\pm} > 0$ ) the deviations between data and nPDF predictions grow. It can be understood in the following way. If we map the rapidity values to the  $x$  of lead nucleus that is probed<sup>3</sup> we find that the negative rapidities correspond to moderate  $x$  values ( $\sim 0.1$ ) and positive rapidities to the low  $x$  values ( $\sim 3 \times 10^{-3}$ ), see Fig. 4. At the same time we know that the low- $x$  range of nPDFs is unconstrained by the data currently used in the nPDF fits, so these results come from an extrapolation of the larger  $x$  region.

It is interesting to observe that a delayed shadowing (which shifts the shadowing down to smaller  $x$  values) would improve the comparison of the

<sup>3</sup> This strictly holds only at leading order.

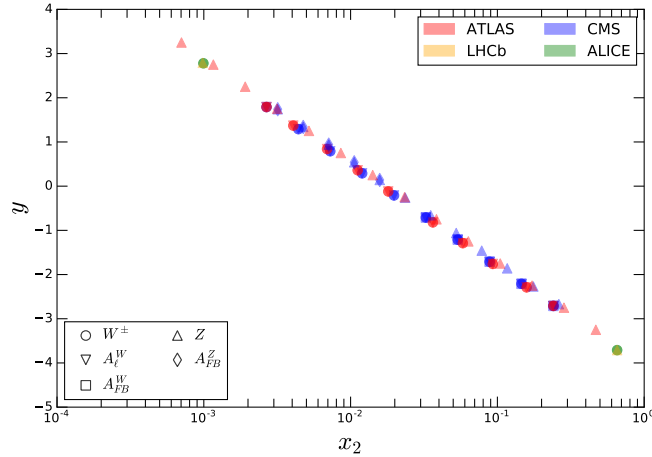


Fig. 4: Kinematic  $x$ -rapidity plane of lead covered by currently available LHC pPb  $W/Z$  production data.

data with the theory in the larger  $y_{l\pm}$  region; this type of behavior was observed in the nuclear corrections extracted from the neutrino-DIS charged current data [24–27]. Taking into account the errors from both the experimental data and the theoretical predictions, no definitive conclusions can be drawn at the present time. Nonetheless, this data has the potential to strongly influence the nPDF fits, especially in the small  $x$  region. This will be even more pronounced with the new data collected at the end of 2016, where nearly 10 times more statistics were recorded.

### 3. Strange contribution

In order to analyze our results more quantitatively, it is very useful to look at PDF correlations. In particular, we are interested in assessing the importance of the strange quark in our results. We will focus here on the correlations between  $W^+$  and  $W^-$  cross sections, a more comprehensive discussion including  $Z$  cross section is presented in [17]. The correlations will be quantified by means of correlation cosine defined in [17, 28]. In our figures they are plotted as ellipses around central predictions for different PDFs.

Fig. 5 shows the correlations of the predicted  $W^+$  and  $W^-$  production cross sections for pPb collisions at the LHC in comparison with the CMS measurements. The same result is displayed in Fig. 6 but split into three different rapidity regions,  $y < -1$ ,  $|y| < 1$ ,  $y > 1$ . For the proton side we always use the CT10 PDFs and for the lead side we examine four cases: i) nCTEQ15, ii) CT10, iii) CT10 PDFs supplemented by the

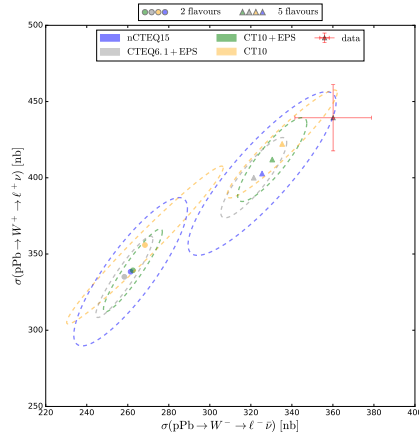


Fig. 5: Comparison of correlations between  $W^+$  and  $W^-$  cross sections for the case when only one family of quarks  $\{u, d\}$  is included and when all families are accounted for.

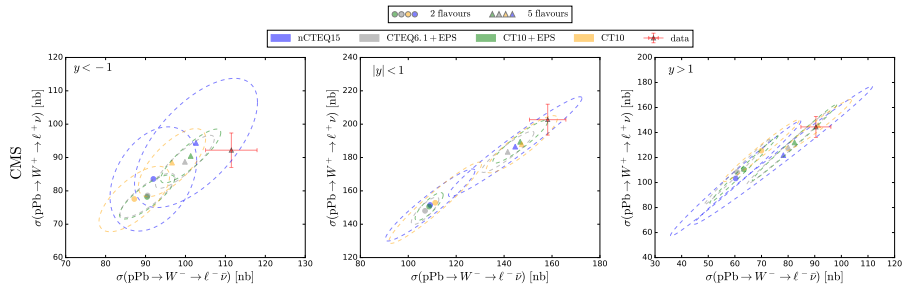


Fig. 6: Same as Fig. 5 but divided into rapidity bins.

nuclear corrections from EPS09 (CT10+EPS09), and iv) CTEQ6.1 proton PDFs supplemented by EPS09 nuclear corrections (CTEQ6.1+EPS09). Additionally, to quantify the contribution of the strange quark we present also results calculated using only 2 quark flavours (one family)  $\{u, d\}$ . In this way we eliminate the contribution from the strange PDF (the c and b PDF contributions are small).

The shift of the 2 flavor results compared to the 5 flavor results can be as large as 30% and reflects the large size of the strange contributions. The strange contributions to  $W/Z$  boson production at the LHC are substantial [29] and are primarily responsible for the observed differences among the nuclear results (nCTEQ15, EPS09+CT10, EPS09+CTEQ6.1). On the other hand, the observed differences between the 2 flavor proton CT10 and

the nuclear (nCTEQ15, EPS09) results accurately represent the nuclear corrections associated with these quantities. Indeed, the nCTEQ15 and EPS09+CTEQ6.1 results are generally very close due to the fact that the CTEQ6.1 and nCTEQ15 baseline PDFs are very similar.

As we review these correlation plots there are a number of general features which we can identify. As we move from negative  $y$  to positive  $y$  we move from high  $x$  where the nPDFs are well constrained to small  $x$  where the nPDFs have large uncertainties (still underestimated). Thus, it is encouraging that at  $y < -1$  we uniformly find the nuclear predictions yield larger cross sections than the proton results (without nuclear corrections) and thus lie closer to the LHC data. Conversely, for  $y > 1$  we find the nuclear predictions yield smaller cross sections than the proton results. This situation suggests a number of possibilities.

First, the large nPDF uncertainties in the small  $x$  region could be improved using the LHC data.

Second, the lower nPDF cross sections are partly due to the nuclear shadowing in the small  $x$  region; if, for example, this shadowing region were shifted to even lower  $x$  values, this would increase the nuclear results. Such a shift was observed in Refs. [24–26] using charged current neutrino-DIS data, and this would move the nuclear predictions at  $y > 1$  toward the LHC data.

Finally, we note that measurements of the strange quark asymmetry [30] indicate that  $s(x) \neq \bar{s}(x)$  which is unlike what is used in the current nPDFs; this would influence the  $W^\pm$  cross sections separately as (at leading-order)  $W^+ \sim \bar{s}c$  and  $W^- \sim s\bar{c}$ . As the strange PDF has a large impact on the  $W^\pm/Z$  measurements, this observation could provide incisive information on the individual  $s$  and  $\bar{s}$  distributions.

#### 4. Impact of the data on nPDFs

Ultimately, to see the impact of the LHC vector boson data on the nCTEQ15 PDFs we will perform a new global analysis including these data. This work is ongoing but in the meantime we try to estimate these effects by employing the reweighting method [31–34].

In this exercise we use the Giele-Keller (GK) weight supplemented by the tolerance criterion  $T$  used in the nCTEQ15 fit

$$w_k = \frac{e^{-\frac{1}{2}\chi_k^2/T}}{\frac{1}{N_{\text{rep}}} \sum_i^{N_{\text{rep}}} e^{-\frac{1}{2}\chi_i^2/T}}, \quad \chi_k^2 = \sum_j^{N_{\text{data}}} \frac{(D_j - T_j^k)^2}{\sigma_j^2}, \quad (1)$$

where  $\chi_k^2$  represents the  $\chi^2$  of the data sets considered in the reweighting procedure for a given replica  $k$ . This definition of the weight has been

shown to reproduce the full Hessian fit [33,34]; as such it is an appropriate choice for PDFs produced using the Hessian framework. More details of the reweighting procedure can be found in our detailed study [17]. Here we only note that after the reweighting, the PDF-dependent observables and their errors can be computed as weighted sums

$$\begin{aligned}\langle \mathcal{O} \rangle_{\text{new}} &= \frac{1}{N_{\text{rep}}} \sum_{k=1}^{N_{\text{rep}}} w_k \mathcal{O}(f_k), \\ \delta \langle \mathcal{O} \rangle_{\text{new}} &= \sqrt{\frac{1}{N_{\text{rep}}} \sum_{k=1}^{N_{\text{rep}}} w_k (\mathcal{O}(f_k) - \langle \mathcal{O} \rangle)^2}.\end{aligned}\tag{2}$$

As an example, we consider the reweighting using the CMS  $W^\pm$  production data from pPb collisions [9] (these data have the smallest uncertainties among the currently available vector boson pPb data). In this example we use rapidity distributions of charged leptons originating from the decay of both  $W$  bosons and we employ  $N_{\text{rep}} = 10^4$  replicas.

In Fig. 7 we show the comparison of the data to theory before and after the reweighting procedure.<sup>4</sup> As expected, we see that after the reweighting procedure the description of the data is improved. This is true for both the  $W^+$  (left panel) and  $W^-$  (right panel) cases. We can quantify the improvement of the fit by examining the  $\chi^2/N_{\text{data}}$  for the individual distributions. For the  $W^+$  case, the  $\chi^2/N_{\text{data}}$  is improved from 5.07 before reweighting to 3.23 after reweighting. Similarly, for  $W^-$  the  $\chi^2/N_{\text{data}}$  is improved from 4.57 to 3.44. The amount of change due to the reweighting procedure should be proportional to the experimental uncertainties of the incorporated data. For  $W^\pm$  production investigated here, the uncertainties are quite substantial, and the effects are compounded by the lack of correlated errors.

Still, even with the current data uncertainties we can see that the improvement of the data description after the reweighting procedure is limited and the resulting  $\chi^2/N_{\text{data}}$  values are not satisfactory. This is caused by considerably underestimated nPDF error bands, especially in the positive rapidity region. As mentioned before, the low  $x$  (large rapidity) region of the current nPDFs is extrapolated as there are no constraints from data prior to the LHC measurements. The underestimation of the errors is a result of too restrictive parametrization form used in the nPDF analyses which, however, is necessary to obtain stable fits.

---

<sup>4</sup> We note here the difference of PDF uncertainties compared to the plots presented in the previous sections. This is caused by the use of the 68% c.l. errors compared to the standard nCTEQ15 90% c.l. errors which were used earlier. This holds for all reweighting plots.



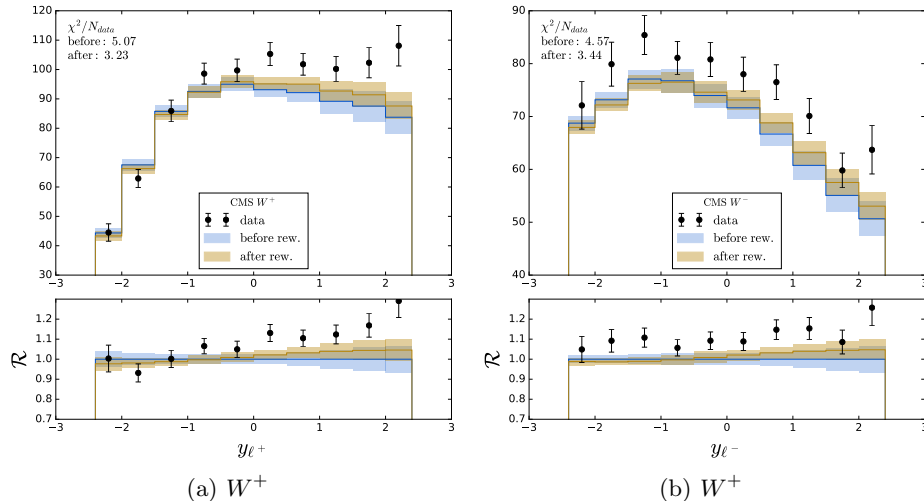


Fig. 7: Comparison of data and theory before and after the reweighting using CMS  $W^\pm$  data for the nCTEQ15 PDFs.

This exercise shows that it is mandatory to release some of the assumptions and use more flexible parameterizations to fully accommodate the vector boson LHC data in nPDF global fits. This is also confirmed by the new EPPS16 analysis [20].

#### 4.1. Strange contribution

We have shown that strange distribution is important for the  $W/Z$  production at the LHC. This clearly suggests that one of the reasons we have difficulties accommodating  $W^\pm$  data in the current reweighting exercise is the lack of proper estimates of strange distribution errors. Due to the lack of data the strange PDF is not fitted in the nCTEQ15 and other nuclear analyses, but it is fixed to be proportional to the light sea distribution  $\bar{u} + \bar{d}$ . We try to address this problem doing a dedicated fit (referred to as strALL2c) where nCTEQ15 analysis is extended by including neutrino di-muon data [35].<sup>5</sup> These data can put limited constraints on the strange allowing us to free some of the corresponding fit parameters, and consequently provide more realistic error bars. This can be seen in Fig. 8 where predictions for the CMS  $W^\pm$  data for this new fit with extra strange flex-

<sup>5</sup> The neutrino di-muon data are often used in proton PDF analyses to constrain strange distribution. They are however, rarely used in the nuclear PDF fits because of the unanswered question about the compatibility of the charge lepton and neutrino nuclear corrections.

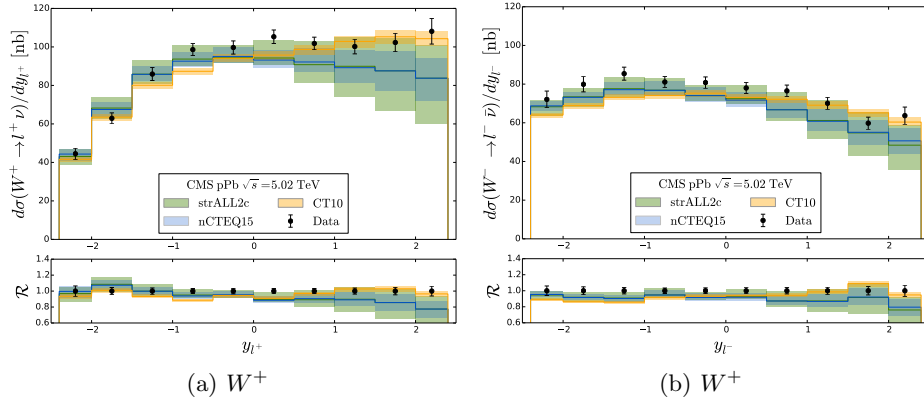


Fig. 8:  $W^\pm$  production in pPb collisions at the LHC from CMS compared with predictions from nCTEQ15, CT10, and strALL2c (nCTEQ15 with additional strange flexibility) PDFs.

ibility is compared to the original prediction for the nCTEQ15 PDFs. We can see a substantial increase of the error bars in the positive rapidity (low  $x$ ) region, this is the extrapolation region, where nuclear PDF errors are underestimated to a large extent.

To finish this exercise we perform a reweighting on the new strALL2c PDFs to see if the additional flexibility allows to obtain more reliable results. In Fig. 9 we present the comparison of the data to theory before and after the reweighting procedure using the strALL2c fit. We can see that, indeed, the extra flexibility in strange distribution (higher errors) allowed for more effective reweighting. The  $\chi^2/N_{\text{data}}$  for  $W^+$  case is now 2.20 and for  $W^-$  it is 3.17. Especially in case of the  $W^+$  boson the improvement compared to the nCTEQ15 reweighting is substantial (over 1 unit per data point).

This result shows that we are going in the right direction, however, the obtained  $\chi^2/N_{\text{data}}$  are still relatively large and new fit with even more flexibility is needed to properly incorporate the LHC vector boson data.

## 5. Conclusions

We have presented a study of vector boson production in lead collisions at the LHC. These data are of particular interest for nPDF determinations. A comparison with the LHC proton data provides a direct probe of nuclear corrections for large  $A$  values in a kinematic  $\{x, Q^2\}$  range very different from the nuclear corrections extracted from fixed-target measurements.

Our study has demonstrated the importance of the strange distribution for the vector boson production at the LHC, possibly even pointing to a

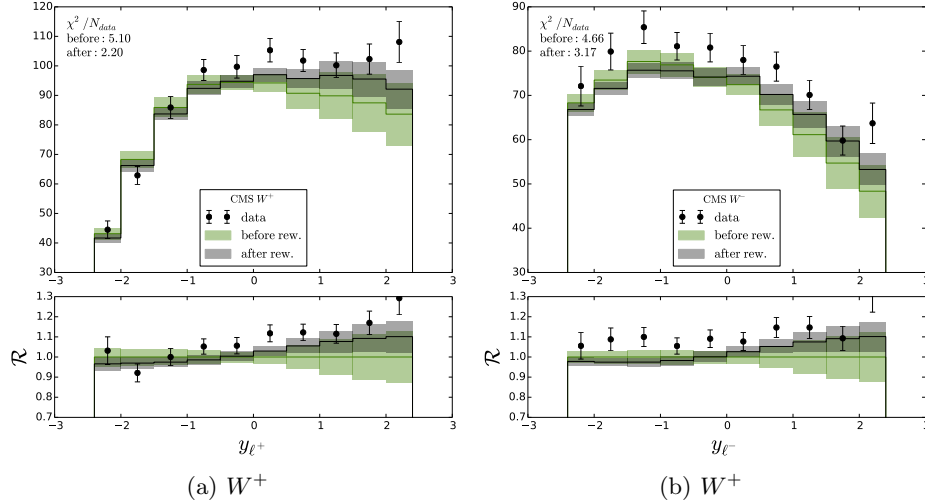


Fig. 9: Comparison of data and theory before and after the reweighting using CMS  $W^\pm$  data for the strALL2c PDFs (nCTEQ15 with additional strange flexibility).

nuclear strangeness asymmetry ( $s(x) > \bar{s}(x)$ ). More importantly, it showed that the currently used nuclear strange distributions are not adequate and the characteristic underestimation of errors can cause problems with the description of the LHC data.

This sensitivity to the strange distribution and heavier flavours can provide important information on the nuclear flavor decomposition, which is invaluable for a precise nPDF determination.

Intriguingly, the large rapidity  $W/Z$  data seem to prefer nuclear PDFs with no shadowing or delayed shadowing at small  $x$ , similar to what has been observed in neutrino DIS.

## REFERENCES

- [1] R. D. Ball *et al.*, “Parton distributions with LHC data,” *Nucl. Phys.* **B867** (2013) 244–289, 1207.1303.
- [2] K. Kovarik *et al.*, “nCTEQ15 - Global analysis of nuclear parton distributions with uncertainties in the CTEQ framework,” *Phys. Rev.* **D93** (2016), no. 8, 085037, 1509.00792.
- [3] K. J. Eskola, H. Paukkunen, and C. A. Salgado, “EPS09: A New Generation of NLO and LO Nuclear Parton Distribution Functions,” *JHEP* **04** (2009) 065, 0902.4154.

- [4] M. Hirai, S. Kumano, and T.-H. Nagai, “Determination of nuclear parton distribution functions and their uncertainties in next-to-leading order,” *Phys.Rev.* **C76** (2007) 065207, 0709.3038.
- [5] H. Paukkunen and C. A. Salgado, “Constraints for the nuclear parton distributions from Z and W production at the LHC,” *JHEP* **03** (2011) 071, 1010.5392.
- [6] **ATLAS** Collaboration, G. Aad *et al.*, “Z boson production in p+Pb collisions at  $\sqrt{s_{NN}} = 5.02$  TeV measured with the ATLAS detector,” *Phys. Rev.* **C92** (2015), no. 4, 044915, 1507.06232.
- [7] **CMS** Collaboration, V. Khachatryan *et al.*, “Study of Z boson production in pPb collisions at  $\sqrt{s_{NN}}=5.02\text{TeV}$ ,” *Phys. Lett.* **B759** (2016) 36–57, 1512.06461.
- [8] **LHCb** Collaboration, R. Aaij *et al.*, “Observation of Z production in proton-lead collisions at LHCb,” *JHEP* **09** (2014) 030, 1406.2885.
- [9] **CMS** Collaboration, V. Khachatryan *et al.*, “Study of W boson production in pPb collisions at  $\sqrt{s_{NN}} = 5.02$  TeV,” *Phys. Lett.* **B750** (2015) 565–586, 1503.05825.
- [10] **ATLAS** Collaboration, “Measurement of  $W \rightarrow \mu\nu$  production in p+Pb collision at  $\sqrt{s_{NN}} = 5.02$  TeV with ATLAS detector at the LHC,” ATLAS-CONF-2015-056.
- [11] **ALICE** Collaboration, K. J. Senosi, “Measurement of W-boson production in p-Pb collisions at the LHC with ALICE,” *PoS Bormio2015* (2015) 042, 1511.06398.
- [12] **ATLAS** Collaboration, G. Aad *et al.*, “Measurement of Z boson Production in Pb+Pb Collisions at  $\sqrt{s_{NN}} = 2.76$  TeV with the ATLAS Detector,” *Phys. Rev. Lett.* **110** (2013), no. 2, 022301, 1210.6486.
- [13] **CMS** Collaboration, S. Chatrchyan *et al.*, “Study of Z production in PbPb and pp collisions at  $\sqrt{s_{NN}} = 2.76$  TeV in the dimuon and dielectron decay channels,” *JHEP* **03** (2015) 022, 1410.4825.
- [14] **ATLAS** Collaboration, G. Aad *et al.*, “Measurement of the production and lepton charge asymmetry of W bosons in Pb+Pb collisions at  $\sqrt{s_{NN}} = 2.76$  TeV with the ATLAS detector,” *Eur. Phys. J.* **C75** (2015), no. 1, 23, 1408.4674.
- [15] **CMS** Collaboration, S. Chatrchyan *et al.*, “Study of W boson production in PbPb and pp collisions at  $\sqrt{s_{NN}} = 2.76$  TeV,” *Phys. Lett.* **B715** (2012) 66–87, 1205.6334.
- [16] N. Armesto, H. Paukkunen, J. M. Penn, C. A. Salgado, and P. Zurita, “An analysis of the impact of LHC Run I protonlead data on nuclear parton densities,” *Eur. Phys. J.* **C76** (2016), no. 4, 218, 1512.01528.
- [17] A. Kusina, F. Lyonnet, D. B. Clark, E. Godat, T. Jezo, K. Kovarik, F. I. Olness, I. Schienbein, and J. Y. Yu, “Vector boson production in proton-lead and lead-lead collisions at the LHC and its impact on nCTEQ15 PDFs,” 1610.02925.

- [18] D. de Florian, R. Sassot, P. Zurita, and M. Stratmann, “Global Analysis of Nuclear Parton Distributions,” *Phys. Rev.* **D85** (2012) 074028, 1112.6324.
- [19] P. Ru, S. A. Kulagin, R. Petti, and B.-W. Zhang, “Study of W and Z Boson Production in Proton-Lead Collisions at the LHC with KP Nuclear Parton Distributions,” 1608.06835.
- [20] K. J. Eskola, P. Paakkinen, H. Paukkunen, and C. A. Salgado, “EPPS16: Nuclear parton distributions with LHC data,” 1612.05741.
- [21] F. Arleo, E. Chapon, and H. Paukkunen, “Scaling properties of inclusive  $W^\pm$  production at hadron colliders,” *Eur. Phys. J.* **C76** (2016), no. 4, 214, 1509.03993.
- [22] H.-L. Lai, M. Guzzi, J. Huston, Z. Li, P. M. Nadolsky, J. Pumplin, and C. P. Yuan, “New parton distributions for collider physics,” *Phys. Rev.* **D82** (2010) 074024, 1007.2241.
- [23] R. Gavin, Y. Li, F. Petriello, and S. Quackenbush, “W Physics at the LHC with FEWZ 2.1,” *Comput. Phys. Commun.* **184** (2013) 208–214, 1201.5896.
- [24] K. Kovarik, I. Schienbein, F. I. Olness, J. Y. Yu, C. Keppel, J. G. Morfin, J. F. Owens, and T. Stavreva, “Nuclear corrections in neutrino-nucleus DIS and their compatibility with global NPDF analyses,” *Phys. Rev. Lett.* **106** (2011) 122301, 1012.0286.
- [25] I. Schienbein, J. Y. Yu, K. Kovarik, C. Keppel, J. G. Morfin, F. Olness, and J. F. Owens, “PDF Nuclear Corrections for Charged and Neutral Current Processes,” *Phys. Rev.* **D80** (2009) 094004, 0907.2357.
- [26] S. X. Nakamura *et al.*, “Towards Construction of a Unified Model for the Neutrino-Nucleus Reactions,” 1610.01464.
- [27] N. Kalantarians, “Comparison of the Iron Nuclear Structure Function  $F_2$  as Measured by Charged Lepton and Neutrino Probes,” *JPS Conf. Proc.* **12** (2016) 010028.
- [28] P. M. Nadolsky, H.-L. Lai, Q.-H. Cao, J. Huston, J. Pumplin, D. Stump, W.-K. Tung, and C. P. Yuan, “Implications of CTEQ global analysis for collider observables,” *Phys. Rev.* **D78** (2008) 013004, 0802.0007.
- [29] A. Kusina, T. Stavreva, S. Berge, F. I. Olness, I. Schienbein, K. Kovarik, T. Jezo, J. Y. Yu, and K. Park, “Strange Quark PDFs and Implications for Drell-Yan Boson Production at the LHC,” *Phys. Rev.* **D85** (2012) 094028, 1203.1290.
- [30] **NuTeV** Collaboration, D. Mason *et al.*, “Measurement of the Nucleon Strange-Antistrange Asymmetry at Next-to-Leading Order in QCD from NuTeV Dimuon Data,” *Phys. Rev. Lett.* **99** (2007) 192001.
- [31] W. T. Giele and S. Keller, “Implications of hadron collider observables on parton distribution function uncertainties,” *Phys. Rev.* **D58** (1998) 094023, hep-ph/9803393.
- [32] **NNPDF** Collaboration, R. D. Ball, V. Bertone, F. Cerutti, L. Del Debbio, S. Forte, A. Guffanti, J. I. Latorre, J. Rojo, and M. Ubiali, “Reweighting NNPDFs: the W lepton asymmetry,” *Nucl. Phys.* **B849** (2011) 112–143, 1012.0836. [Erratum: *Nucl. Phys.*B855,927(2012)].

- [33] H. Paukkunen and P. Zurita, “PDF reweighting in the Hessian matrix approach,” *JHEP* **12** (2014) 100, 1402.6623.
- [34] N. Sato, J. F. Owens, and H. Prosper, “Bayesian Reweighting for Global Fits,” *Phys. Rev.* **D89** (2014), no. 11, 114020, 1310.1089.
- [35] **NuTeV** Collaboration, M. Goncharov *et al.*, “Precise measurement of dimuon production cross-sections in muon neutrino Fe and muon anti-neutrino Fe deep inelastic scattering at the Tevatron,” *Phys. Rev.* **D64** (2001) 112006, hep-ex/0102049.